Design and Development of a Remote-Control Test Bench for Remote Piloted Aircraft's Brushless Motors

Tiberius-Florian FRIGIOESCU, Teodor-Adrian BADEA, Mihaela Raluca CONDRUZ, Grigore CICAN*, Ionel MÎNDRU

Abstract: The present paper is focused on designing and manufacturing a remote-control test bench for RPA's brushless motors. The main components of the testing bench (structural, mechanical and electric components) are presented, how they are coupled, and the operating principle. The test bench is characterized by five emergency systems, one manual and four automated emergency systems that can stop the test under different conditions to avoid damaging the motor. To validate the testing bench, a SK3-5045 660 kV electric motor was selected along with a carbon fibre reinforced composite propeller. It was experimentally demonstrated that the test bench was fully automated, there were measured the propulsion force, current intensity, voltage, but also the consumed power of a motor intended for an RPA. The test results were used to determine the motorization performance and power consumption of an RPA designed with four electric motors (quadcopter type).

Keywords: aircraft; brushless motors; RPAS; sensors; test bench

1 INTRODUCTION

Nowadays, an increased interest in unmanned aerial systems (UAS) is registered for both civil and industrial fields, thereby they present a challenge for the integration in the non-segregated airspace along with manned aircraft [1, 2], especially for the Air Traffic Control (ATC). Many terms are used to refer to an UAS. Depending on the nation and organization that use them, terms like remotely piloted aircraft (RPA) or remotely piloted aircraft systems (RPAS), and drones are reported [3]. Even if there is a distinction between those terms, what they all have in common is that they imply an aerial vehicle that operates without a human operator on board. According to the International Civil Aviation Organization (ICAO), only the unmanned aircrafts that are remotely piloted will be integrated alongside manned aircrafts in non-segregated airspace and at airdromes, excluding the fully autonomous or combined options [4].

The advantages of using RPA are obvious, they offer new capabilities for the deployment of sensors for various applications, including science, logistics, education, journalism, and recreational activities. They are a more cost-effective method compared with a conventional aircraft [5]. The RPAs have been successfully applied in wildlife monitoring and wooded vegetation study [6] as a way to improve or supplement conventional field observations [7, 8]. They are a safe method to study fierce wild animals (i.e. the Nile crocodile [9]) or to discover poachers [10, 11]. It was reported that RPAS can also be used for the infrared imaging of photovoltaic systems, a more cost-effective approach than conventional techniques [12]. Besides these fields, the RPAs were used in the wind energy field where they were deployed to retrieve information about the flow field, turbulence intensity, vertical wind components and shear at the escarpment site [13]. Other fields that benefit from the advantages of RPA are the archaeological and agricultural field, and cartography where RPA were used for surveillance and aerial photography [14-16]. Except for these applications, they were deployed for structural safety inspections, such as buildings and bridges with high seismic risk [17].

Many types of RPAs were developed [18, 19], but most of them use propellers and are powered by electric motors (brushed or brushless DC motors). In terms of stability, two types of RPA can be mentioned: fixed and rotor-wing aircraft. The most popular type of RPA are the rotor-wing aircrafts; they are characterized by a high degree of freedom in terms of rotor number, such as bicopters, tricopters, quadcopters, hexacopters, and octocopters. They are characterized by high reliability [20] and are adequate for uneven and inhomogeneous grounds [21].

As many RPAs are powered by electric motors, during the design phase it is important to test the electrical configuration of the RPA to define the operating parameters and to avoid the damage to the motor or other components. Studies have been conducted regarding testing and data acquisition during testing of electric motors for RPAs [22-24] as many test benches have been developed [25, 26]. The patented test benches [25, 26] have several disadvantages, but the main disadvantage is that they are not remote controlled and a human operator must control and supervise them throughout the testing campaign.

The present study was focused on designing and manufacturing a low-cost, remote control test bench for brushless motors used in RPAs. The goal of this bench was to determine the performance and limitations of an electric motor configuration designed for an RPA. The configuration presented in this study was used to obtain a utility model.

2 DESIGNING AND MANUFACTURING OF THE TEST BENCH
2.1 Test Bench Description

An automated test bench was designed and manufactured to automatically test a RPA motor configuration. In reference [27] a universal experimental measuring system for more accurate measurement of propeller's parameters was presented.

By design, the test bench had to fulfil the following functions:
• testing a brushless motor with a propeller,

•automatic measurement and recording of the generated propulsion force,
• autonomous control of motor speed,
• remote control,
• manual control for emergency motor shutdown,
• automatic emergency system to stop the motor in case of propeller detachment,
• automatic emergency system to stop the motor in case of exceeding the maximum force of the load cell,
• automatic emergency system to stop the motor in case its maximum power is exceeded,
• automatic emergency system to stop the motor in case it exceeds the maximum current intensity of the electronic speed controller (ESC),
• register and export data such as *PWM* percentage, current intensity, voltage, force, power, and speed in an excel file.

During the design phase of a rotor-wing RPA, many factors should be considered. For example, the battery ESC propeller configuration must be selected in a way that the electric motor should reach the required thrust-weight ratio. Moreover, the propeller selection is important, it is a component with a significant role, it provides the propulsive force by spinning at a speed range and sets the consumed power of the RPA.

The power consumption has to be lower than the electric motor's maximum power, and the motor should be able to provide the required speed range for the propeller. Besides, the ESC should be selected to comply with the motor voltage and its required amperage, and the battery should provide the voltage and amperage required for the configuration. Therefore, the *PWM* signal should not exceed the value at which the power consumption is higher than the motor capacity by driving the propeller at higher speeds. A higher value compared to the motor's power and an amperage higher than the maximum limit of the ESC can damage the motor and ESC.

The test bench consists of a clamping frame made of rolled steel angles, as can be seen in the images from Fig. 1.
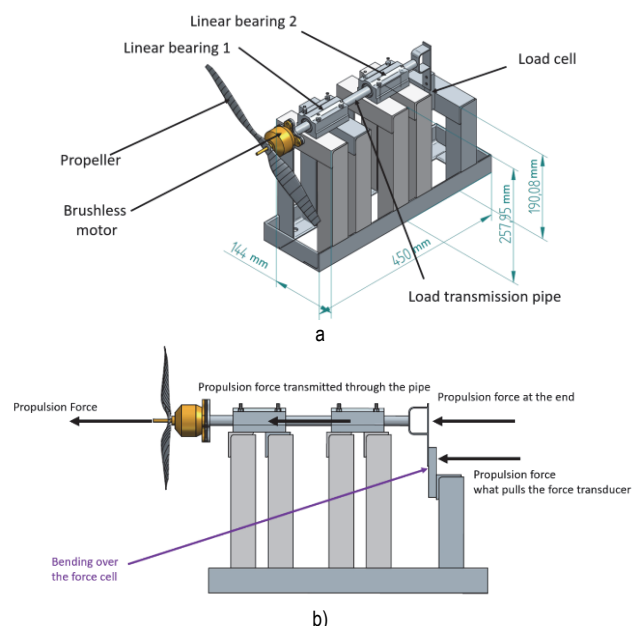

Figure 1 The graphic representation of the testing bench: (a) components; (b) the working principle of the test bench

The metallic skeleton was fastened to a solid table using four screws; two linear bearings were attached with screws to the metallic frame. A 16 mm in diameter metallic pipe passes through the two linear bearings; it is a force transmission pipe. These bearings are used to block the pipe and to allow it to slide only on their axis also eliminating friction during testing.

At one extremity of the pipe, a flange was mounted using four screws, and at the other extremity a metallic part was welded. This metallic part was connected with screws to the load cell. In this configuration, the load cell was mounted at one extremity of the pipe to be pulled at the other extremity with an equal force to the propulsion force generated by the propeller during testing.

The brushless motor selected for the validation of the test bench was a SK3-5045 660 kV motor with a maximum power of 1410 W and an operational voltage of 4-5S meaning 4 - 5 × 3.7 V. The motor was powered by a LiPo battery with a 16000 mAh 6S capacity and a discharge capacity of 12 - 24 C. Some RPAs use Li-Ion batteries because they are reliable and the most available battery technology [28], but other RPAs use the LiPo batteries because they have a high discharge capacity compared to Li-Ion batteries and can provide a high current intensity required for brushless electric motors [29].

A carbon fibre reinforced polymer propeller was attached to the motor; it was 381 mm in diameter and had a pitch of 139.7 mm. As the motor is mounted on the test bench using a flange, when it starts, it pulls the flange that activates the load cell. During testing, the load cell is subjected to bending, the bending force is registered by an electrical resistor that sends an electrical signal to the HX711 decoder. Afterwards, the decoder reads the electrical signal and provides the value of the force.

2.2 Operating Block Diagram of the Test Bench

In the block wiring diagram of the test bench, three individual electrical circuits are available:
• an electrical circuit for the power supply of the electric motor, primary circuit,
• an electrical circuit for the first Raspberry Pi (further called R1),
• an electrical circuit for the second Raspberry Pi (further called R2).

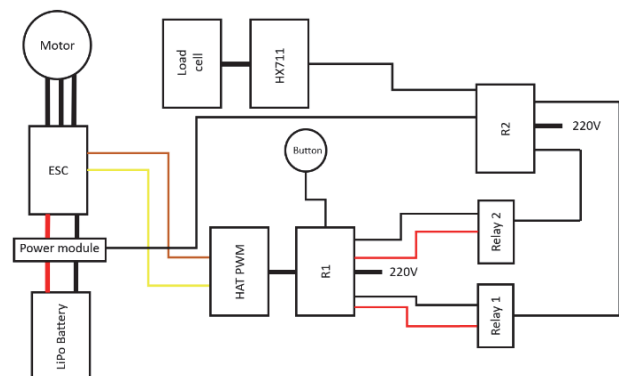The block diagram of the test bench's wiring is presented in Fig. 2.

Figure 2 The block diagram of the test bench's wiring

In the primary circuit, the LiPo battery transmits DC to the ESC. The ESC controls the voltage and amperage generated to the electric motor in the form of alternating current (AC) depending on the received *PWM* signal.

The R1 circuit integrates a button, a *PWM* hat, the ESC and two relays. The *PWM* hat increases the control accuracy of the *PWM* signal generated by the ESC. The button is attached to two general purpose input/output (GPIO) pins, one that sends a signal continuously, and the other pin waits for the electrical signal. By pressing the button, the circuit closes.

Also, a GPIO pin sends a continuous signal to a COM socket of a relay 1. Another GPIO pin is attached to this relay 1 in the NO socket. This means that when relay 1 is not supplied with an electric current of 5 VDC, the circuit between COM and NO is open (there is no electric current between them). The same circuit also exists for the second relay (relay 2).

The R2 circuit is in charge of the load cell that is read through the HX711 decoder. It also is in charge of powering the relays 1 and 2, and of reading the power module. Both R1 and R2 are powered by a conventional 220 VAC voltage. In Fig. 3 is presented an image with the electrical test bench components.
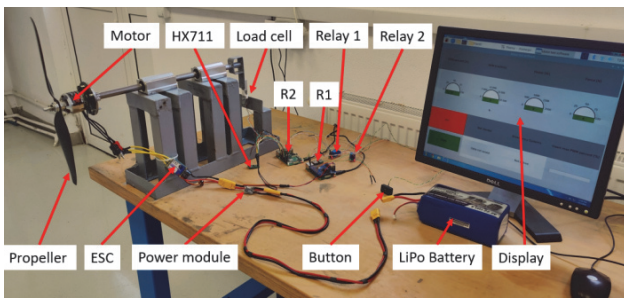

Figure 3 Test bench electric components

2.3 Test Bench Software Interface

The scripts used by the testing bench were realized using the Python Programming Language. They were realized based on different diagrams like the one presented in Fig. 4, which is used by the R1 circuit.
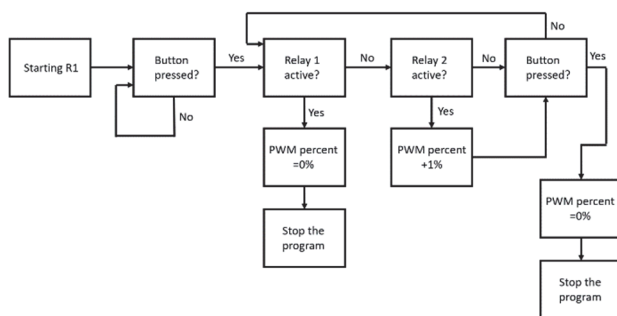

Figure 4 The diagram used for the programming script of R1 circuit

The script is in charge of the electric motor according to the signals received from R2 circuit. To run the script, first the safety button must be manually pressed. After pressing the button, the script performs a security check in a loop, it checks if the relay 1 and 2 are active or if the button is pressed. If relay 1 is active, the script will send a *PWM* signal to the ESC that sets the motor speed to 0 and

the program stops. If relay 2 is active, the script will increase the engine speed by 1% (*PWM* percentage). Also, if the button is pressed, the engine speed will be set to 0 and the program will close. The operating diagram according to which the script for the R2 was written is shown in Fig. 5.
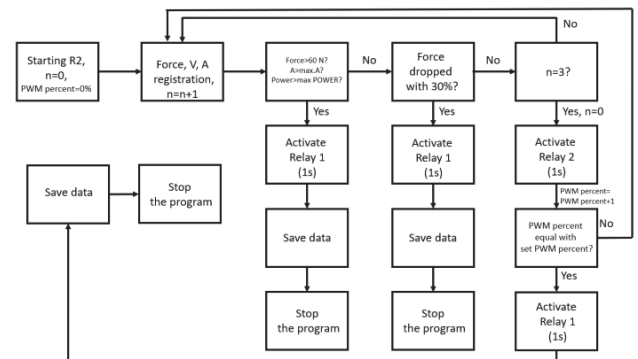

Figure 5 The diagram used for the programming script of R2 circuit

The test bench has five emergency systems: four automatic and one manual, as follows:
• Automatic emergency system 1: If the registered force exceeds the value of 60 N, then the motor will stop instantly and the data will be saved.
• Automatic emergency system 2: If the force suddenly decreases by 30% compared to a measurement value determined in a previous *PWM* percentage, then the motor will stop instantly and the data will be saved (i.e., in case that the propeller breaks or detaches from the motor this emergency system will be activated).
• Automatic emergency system 3: If the amperage exceeds the maximum value of the ESC, then the motor will stop instantly and the data will be saved.
• Automatic emergency system 4: If the power exceeds the maximum power of the motor, then the motor will stop instantly and the data will be saved.
• Manual emergency system: By pressing the button, the engine will stop instantly and the data will be saved.

The script for the R2 circuit represents the command, control and registration centre of the test bench. It performs three force measurements (with a frequency of 1 Hz) at each speed percentage, reads the intensity in the power module, calculates the power and speed and checks after each measurement if the force is greater than 60 N or if it has suddenly decreased by 30% compared to the previous value recorded for a lower *PWM* value. If this happens, the script will activate relay 1 (emergency relay), which will cause the R1 script to stop the motor. In case of an emergency, all the data will be saved. Three force measurements are made, the script activates relay 2, the relay that activates the R1 Raspberry Pi to increase the *PWM* percentage of the motor by 1%. The script is in a loop and if the percentage of *PWM* becomes equal to the initially imposed value, the script will activate relay 2, the motor will stop and the data will be saved. The *PWM* percentage, the measured force, intensity and voltage, speed and power consumed are recorded vectorially so that at the end of each test they are automatically exported to an excel file.

Based on all the information presented it can be concluded that the designed test bench is automated and autonomous. At the beginning of the test, the maximum

PWM percentage, the maximum motor power, the maximum ESC amperage and the voltage vector are introduced depending on the *PWM* percentage taken from a pre-test. After entering this parameter, the program will wait for the button to be pressed to allow it to proceed. Before starting the test, a visual inspection must be made.

After pressing the button, the test stand will increase the motor speed by increasing the *PWM* signal by 1% and the three measurements will be made for each increase in the *PWM* signal. After increasing the *PWM* signal, the program will take a pause (approximate 1 s) for the motor speed to stabilize and to avoid force measurements in the transient regime of the motor. The test ends successfully when the value of the *PWM* percentage becomes equal to the maximum *PWM* percentage entered at the beginning of the test.

The test bench is completely automated and it can also be controlled remotely. Both the R1 and R2 Raspberry Pi are connected to the internet and can be controlled via another PC connected to the internet. Their control is performed by remote-control software, in this case using the VNC Viewer.

Based on the block diagrams, the program code was written and a graphical interface was created to serve the tests. In the image from Fig. 6, is presented the graphical interface of the test stand during a test.

Figure 6 Graphical interface of the test bench

3 LOAD CELL CALIBRATION

Calibration is an important process and was performed after the test bench was manufactured, before starting the testing campaign. The calibration involved fixing the load cell and pulling it with a known force. Depending on this known force, the correction factor on the resulting electrical signal was applied.

The calibration procedure involves the following steps:
• installation of the calibration support,
• starting the registration of the load cell,
• attaching the weight to the wire that passes through the pulley and is connected to the motor flange,
• recording the value registered by the load cell and manually introducing it in the reading script according to the calibration equation. For the calibration procedure, reference [30] was consulted.

To calibrate the load cell, all test bench components were assembled except for the motor and propeller. Instead of a motor, a calibration support was attached. It consists of a metal frame where a pulley is mounted, as can be observed in Fig. 7.
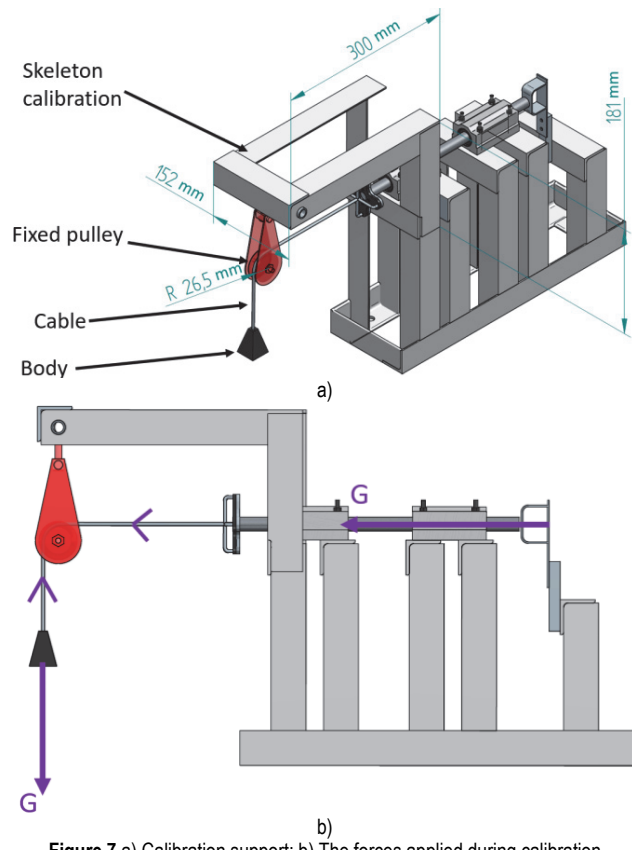

a)

b)
Figure 7 a) Calibration support; b) The forces applied during calibration

A cable was connected to the motor-fixing flange, it passes through the pulley and at the other end of the cable a weight with a known mass was attached.

Due to the gravitational force, the weight will pull the cable, the pulley will transpose the vertical force to horizontal and the cable will pull the motor flange, thereby activating the mechanical system of the load cell with a force equal to the mass of the weight. Thereafter, a correction factor is calculated and applied to the software.

4 EXPERIMENTAL TESTING AND TEST RESULTS-VALIDATION OF THE TEST BENCH

First there was realized the calibration of the load cell. The calibration support was installed on the test bench as can be observed in the image from Fig. 8.

The load cell has a maximum capacity of 20 kg, thereby it was decided to realize the calibration using half of its capacity (10 kg). After calibration, the calibration support was removed, the ESC was connected to the battery, and the testing campaign began.

The testing campaign consisted in performing two pre-tests to determine the scripts functionality, to synchronize the *PWM* signal with the motor start, and to determine the voltage between the motor and the ESC as a function of *PWM*. After the two pre-tests, two tests were performed to evaluate the repeatability of experiments.
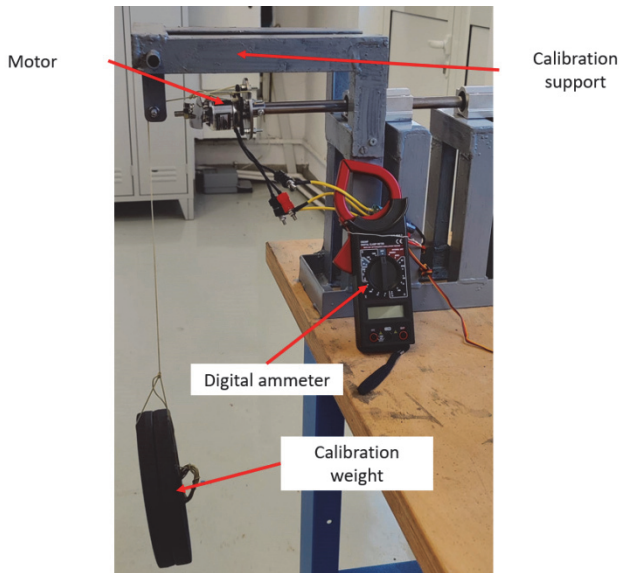
Figure 8 Test bench calibration

The pre-tests were performed using the electrical motor without the propeller. It was experimentally determined that during pre-testing the motor was in the stand-by state at a *PWM* value of 4300, and had a maximum *PWM* value of 8000. Moreover, it was determined that at 4000 *PWM* the motor was in an engine brake state. Based on these measurements, it was determined that as a function of *PWM*, the motor stand-by state corresponded to the 37 step (0% - 100% *PWM* percentage). The following step in the pretesting was the assessment of the script functionality by:
• checking the motor speed increase by increasing the *PWM* percentage,
• checking the emergency stop button,
• checking the emergency system 1,
• checking the emergency system 2,
• checking the program completion,
• checking for the conformity of data saving module.

To check the emergency systems, as the motor was working during pre-testing without the propeller and no propulsive force was generated, a manually electronic weighing scale was used to simulate the increase in the propulsion force up to 60 N or its sudden decrease by 30%. The motor was set to start at 0% *PWM*, the *PWM* setting was realized according to Eq. (1):

$$PWM = Neutral + 37 \cdot Percent \tag{1}$$

where *PWM* is the value of the *PWM*, Neutral is the value of the *PWM* when the motor is in stand-by (in our case 4300 *PWM*), Percent is the desired *PWM* percentage value.

To start the motor the *PWM* percentage was increased to 100% corresponding to the maximum value of the motor. To increase the *PWM* percentage, 1% steps were used with a standing-by time for each step of 5 s. During this standing-by time, the voltage was measured at two of the three terminals of the motor, in the area between the motor and ESC (an area with AC). As the motor speed is a function of voltage and it is specific for each type of motor, the Eq. (2) follows [31]:

$$RPM = U \times KV \tag{2}$$

where *RPM* is the motor speed (rot/min), *U* is the voltage applied to the motor (V), and *KV* is a motor property specified by the producer (in our case 660).

By performing this measurement for each *PWM* percentage, the motor voltage was determined according to the required *PWM* signal. Also using Eq. (2) it was possible to correlate the motor speed according to the applied voltage, by default the *PWM* values. The voltage evolution as a function of the *PWM* value is presented in the graphic from Fig. 9, while the motor speed evolution as a function of the *PWM* value is presented in the graph from Fig. 9a. For these graphs the Excel data provided by the test bench were used as input data, and they were realized using Matlab R2020a.

Knowing the motor speed and the propeller diameter of 381 mm, the speed at the propeller's tip can be calculated according to Eq. (3) [32].

$$V = 2\pi \frac{D}{2} \times \frac{RPM}{60} \tag{3}$$

where *V* is the speed at the propeller's tip (m/s), and *D* is the propeller's diameter (m).

For a better evaluation, an analysis was made as a function of the Mach number. The Mach number was calculated using Eq. (4) where the sound speed was considered 340 m/s.

$$M = \frac{V}{340} \tag{4}$$

where *M* is the Mach number, and *V* is the speed at the propeller's tip (m/s).

The representation of the Mach number calculated as a function of *PWM* is presented in the graph from Fig. 9c.

Based on the results obtained, it can be observed that the motor at 100% *PWM* (the maximum speed) has a 0.73 Mach. Following the pretesting campaign, the actual testing campaign was performed.

For experimental validation of the test bench the motor with the propeller mounted was used. The tests were performed in different days.

During these tests, the motor speed was determined by multiplying the known voltage for each *PWM* percentage with the motor parameter 660 kV. The current intensity recorded was used to determine the power consumption for each *PWM* percentage, thereby the RPA autonomy can be determined along with the power consumption for each propeller. The imposed condition is that this power consumption should not exceed the maximum power of the electrical motor and the current should not exceed the maximum current of the ESC to estimate the motor and propeller performance while not damaging the motor, ESC and battery.

The first test involved increasing the percentage of *PWM* from 0 to 100% with a step of 1%, with three force recordings at each step. An ammeter with a clap was installed to measure the intensity of the AC to check the registered data. It was installed on a wire between the motor and ESC. The *PWM* percentage was displayed on the monitor. The test was started and ended with automatic emergency shutdown by the fact that the force exceeded

60 N. The percentage value of the *PWM* at which the test was stopped was 80%. Therefore, data were taken from 0% to 80% *PWM* percentage.
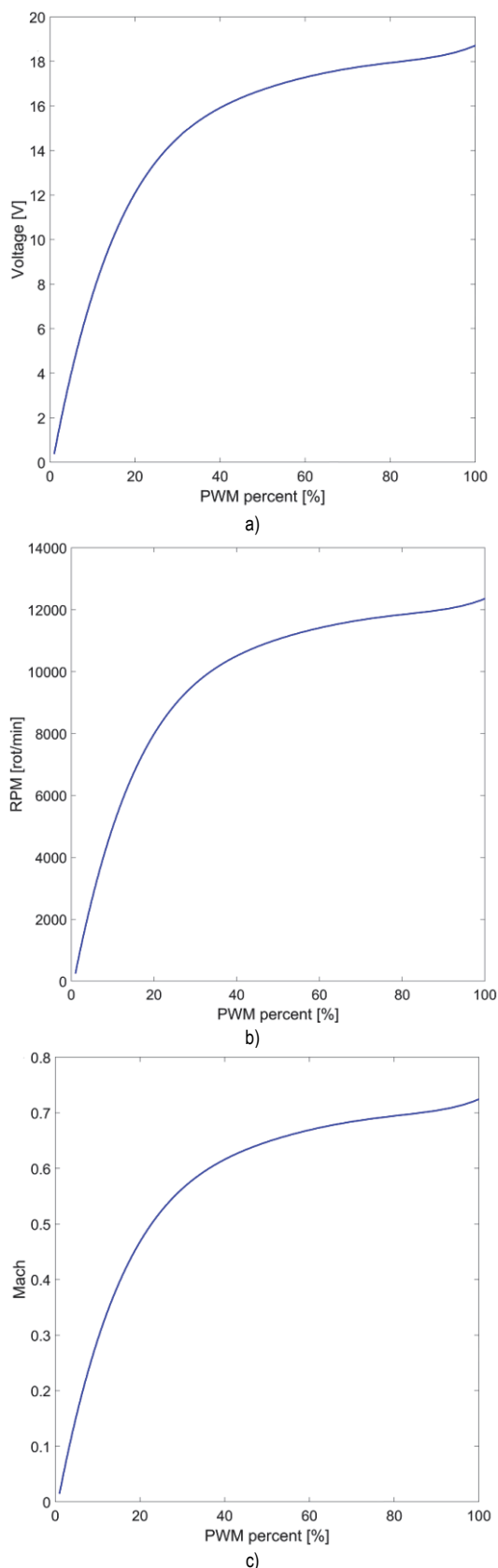

Figure 9 a) Voltage evolution as a function of *PWM* percentage, b) Motor speed evolution as a function of *PWM* percentage, c) Mach number evolution as a function of *PWM* percentage

The second test was performed to evaluate the repeatability of the measurement and was realized from 0% to 70% *PWM* percentage. These values were selected to maintain a safe range for the components. The percentage of 70% corresponds to an amperage of 69 A, and a power of approximately 1220 W, according to the previous test. The propulsion force evolution during testing is presented as a function of *PWM* in the graph from Fig. 10.

It is observed that at 70%, the propulsion force reached is about 50 N. The differences between the curves are given by the axial decentralization of the axial bearings and by the non-uniformity of the pipe passing through them, at 70% this difference is about 3 N. The graph from Fig. 11 shows the evolution of the power consumed to drive the propeller as a function of the motor speed.
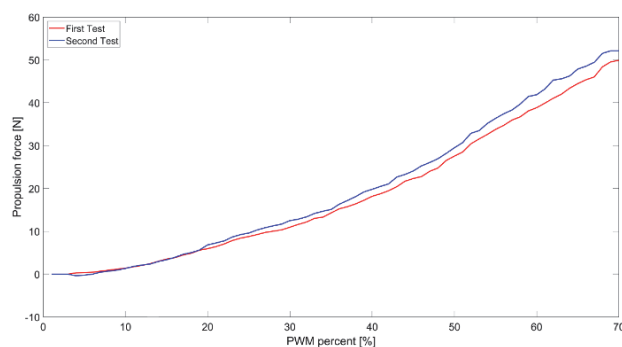

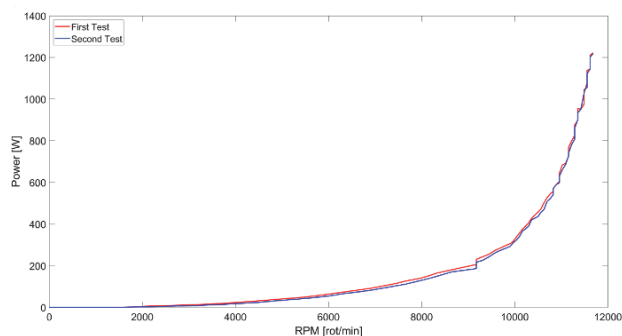**Figure 10** The propulsion force evolution as a function of *PWM*

Figure 11 The consumed power that engages the propeller as a function of the motor speed

The results obtained showed that at a value of 70% *PWM*, a current intensity of 69 A was obtained in the first test and 68.8 A in the second test. Also, an approximate power consumption of the 1221 W propeller (1218 W in the second test) was recorded. Therefore, this coupling version of the electric motor with this propeller and with the ESC, must be limited to a maximum *PWM* percentage of about 78%, because the motor has a maximum power of 1410 W, after which the coils insulator starts to melt and the ESC has a maximum amperage of 80 A.

Therefore, using this test bench, it was found that the propeller should not be limited because in this speed range, it does not enter the transonic regimen, and the engine should be limited to a maximum *PWM* percentage of 78% to not burn the motor or ESC, which is limited by the maximum power. Following the tests, essential data were collected on the propulsion force generated by the engine in the current configuration, its power consumption according to the percentage of *PWM* and the necessary

limitations to be imposed in the operation of this configuration.

5 DISCUSSIONS

The literature survey revealed a high interest for RPAS development and integration in many civil and industrial fields. Many RPA can be found on the market, but they are also built to tailor their capabilities for a specific purpose. During the design and manufacturing stages of an RPA, many testing campaigns should be performed to select the optimum materials for manufacturing, the electric configuration, the motorization, etc. As it was observed many studies were conducted on tests performed on electric motors [22-24] and many test benches were developed for such purpose [25, 26]. The main disadvantage of the existing testing benches is that they are not remote controlled and a human operator must control and supervise them throughout the testing campaign.

Thereby, a new low cost and automated test bench for brushless motors was designed and developed. The automation of this test bench involves recording data and increasing the *PWM* value by a certain autonomous step toward a maximum-desired percentage (imposed). Also, automation is provided by the emergency systems that include stopping of the motor if a certain value of force is exceeded, if the propeller breaks or detaches, or if the limits of the components are exceeded. There is also a manual option to stop the motor through a button 10 m away from the stand. The remote part assumes that the test bench can be mounted on a fixed table in a certain room and its control is done through the internet. Moreover, it is realized using a limited budget; it is a cost-effective version.

6 CONCLUSION

Based on the results presented, it can be concluded that the designed test bench is automated, it can be reached via internet (remotely accessed) and can be used to test brushless DC motors with a propeller mounted in a safe environment.

During the testing campaign, it was observed that the selected motor coupled with the carbon fibre composite propeller, and ESC of 80 A, can be tested up to a maximum *PWM* percentage of 78%, reaching a maximum force at this value of 56 N.

The tested motor configuration will be used in an RPA (quadcopter type) up to a maximum *PWM* percentage of 70% to avoid motor damage. Therefore, the RPA will have a maximum force of 212 N (4 engines like the one tested on the testing bench) and a maximum power consumption of 4868 W. The power consumption on the hover flight will be 3021 W (755 W/engine) with an approximate generating force of propulsion of 30 N on each engine.

This work presents a low-cost test bench that can be used to assess the performances of an electric RPA propulsion system in maximum safety conditions due to the proposed configuration and the programmed algorithm that ensures an autonomous test, without the intervention of an operator. The main advantage of this test bench is related to the autonomous testing of different propulsion system configurations, without risking the entire aircraft. The electric propulsion systems tested can be designed for many RPAS intended for various type of applications, especially in the research field.

Nomenclature

RPA - remotely piloted aircraft
RPAS - remotely piloted aircraft systems
UAS - unmanned aerial systems
ATC- air traffic control
ICAO - International Civil Aviation Organization
DC - direct current
ESC - electronic speed controller
PWM - pulse width modulation
AC - alternating current
GPIO - general purpose input/output
COM - common
NO - normally open

7 REFERENCES

[1] Finke, M. & Lorenz, S. (2020). Segmented Standard Taxi Routes A New Way to Integrate Remotely Piloted Aircraft into Airport Surface Traffic. *Aerospace*, 7, 83. https://doi.org/10.3390/aerospace7060083

[2] Gómez-Rodríguez, A., Sanchez-Carmona, A., García-Hernández, L., & Cuerno-Rejado, C. (2019). Remotely Piloted Aircraft Systems conceptual design methodology based on factor analysis. *Aerospace Science and Technology*, 90, 368-387. https://doi.org/10.1016/j.ast.2019.04.041

[3] https://assets.publishing.service.gov.uk/government/uploads/system/uploads/attachment_data/file/673940/doctrine_uk_uas_jdp_0_30_2.pdf

[4] https://skybrary.aero/sites/default/files/bookshelf/4053.pdf

[5] Kudo, H., Koshino, Y., Eto, A., Ichimura, M., & Kaeriyama, M. (2012). Cost-eective accurate estimates of adult chum salmon, Oncorhynchus keta, abundance in a Japanese river using a radio-controlled helicopter. *Fish. Res.*, *119-120*, 94-98. https://doi.org/10.1016/j.fishres.2011.12.010

[6] Barnetson, J., Phinn, S., & Scarth, P. (2019). Mapping woody vegetation cover across Australia's arid rangelands: Utilising a machine-learning classification and low-cost Remotely Piloted Aircraft System. *Int J Appl Earth Obs Geoinformation, 83*, 101909. https://doi.org/10.1016/j.jag.2019.101909

[7] Hyun, C. U., Park, M., & Lee, W. Y. (2020). Remotely Piloted Aircraft System (RPAS)-Based Wildlife Detection: A Review and Case Studies in Maritime Antarctica. *Animals*, 10, 2387. https://doi.org/10.3390/ani10122387

[8] Harris, C. H., Herata, H., & Herte, F. (2019). Environmental guidelines for operation of Remotely Piloted Aircraft Systems (RPAS): Experience from Antarctica-Review, *Biological Conservation*, *236*, 521-531. https://doi.org/10.1016/j.biocon.2019.05.019

[9] Ezat, M. A., Fritsch, C. J., & Downs, C. T. (2018). Use of an unmanned aerial vehicle (drone) to survey Nile crocodile populations: A case study at Lake Nyamithi, Ndumo game reserve, South Africa. *Biol. Conserv.*, *223*, 76-81. https://doi.org/10.1016/j.biocon.2018.04.032

[10] Mulero-Pázmány, M., Stolper, R., van Essen, L. D., Negro, J. J., & Sassen, T. (2014). Remotely piloted aircraft systems as a rhinoceros anti-poaching tool in Africa. *PLoS ONE*, 9. https://doi.org/10.1371/journal.pone.0083873

[11] Rey, N., Volpi, M., Joost, S., & Tuia, D. (2017). Detecting animals in African Savanna with UAVs and the crowds. *Remote Sens. Environ.*, *200*, 341-351. https://doi.org/10.1016/j.rse.2017.08.026

[12] Rahaman, S. A., Urmee, T., & Parlevliet, D. A. (2020). PV system defects identification using Remotely Piloted Aircraft (RPA) based infrared (IR) imaging. *Solar Energy*, *206*, 579-595. https://doi.org/10.1016/j.solener.2020.06.014

[13] Wildmann, N., Bernard, S., & Bange, J. (2017). Measuring the local wind field at an escarpment using small remotely-piloted aircraft. *Renewable Energy*, *103*, 613-619. https://doi.org/10.1016/j.renene.2016.10.073

[14] Ahmad, A., Ordoñez, J., Cartujo, P., & Martos, V. (2021). Remotely Piloted Aircraft (RPA) in Agriculture: A Pursuit of Sustainability. *Agronomy*, *11*. https://doi.org/10.3390/agronomy11010007

[15] Rani, A., Chaudhary, A., Sinha, N., Mohanty, M., & Chaudhary, R. (2019). Drone: The green technology for future agriculture. *Har. Dhara*, *2*, 3-6

[16] Contreras-de-Villar, F., García, F. J., Muñoz-Perez, J. J., Contreras-de-Villar, A., Ruiz-Ortiz, V., Lopez, P., Garcia-López, S., & Jigena, B. (2021). Beach Leveling Using a Remotely Piloted Aircraft System (RPAS): Problems and Solutions. *J. Mar. Sci. Eng.*, *9*. https://doi.org/10.3390/jmse9010019

[17] Nettis, A., Saponaro, M., & Nanna, M. (2020). RPAS-Based Framework for Simplified Seismic Risk Assessment of Italian RC-Bridges. *Buildings*, *10*. https://doi.org/10.3390/buildings10090150

[18] Vroegindeweij, B. A., van Wijk, S. W., & van Henten, E. (2014). Autonomous unmanned aerial vehicles for agricultural applications. *Proceedings of the Ag Eng*, Zurich, Switzerland.

[19] Pino, E. (2019). Los drones una herramienta para una agricultura eficiente: Un futuro de alta tecnología. *Idesia (Arica)*, *37*, 75-84. https://doi.org/10.4067/S0718-34292019005000402

[20] Agrawal, K. & Shrivastav, P. (2015). Multi-rotors: A revolution in unmanned aerial vehicle. *Int. J. Sci. Res.*, *4*, 1800-1804. https://doi.org/10.21275/v4i11.NOV151540

[21] Sarkisov, Y. S., Yashin, G. A., Tsykunov, E. V., & Tsetserukou, D. (2018). Dronegear: A novel robotic landing gear with embedded optical torque sensors for safe multicopter landing on an uneven surface. *IEEE Robot. Autom. Lett.*, *3*, 1912-1917. https://doi.org/10.1109/LRA.2018.2806080

[22] Motahhir, S., El Hammoumi, A., El Ghzizal, A., & Derouich, A. (2019). Open hardware/software test bench for solar tracker with virtual instrumentation. *Sustainable Energy Technologies and Assessments*, 31, 9-16. https://doi.org/10.1016/j.seta.2018.11.003

[23] Leisten, C., Jassmann, U., Balshüsemann, J., Hakenberg, M., & Abel, D. (2017). Design and Analysis of a MPC-based Mechanical Hardware-in-the-Loop System for Full-Scale Wind Turbine System Test Benches. *IFAC-PapersOnLine*, *50*(1), 10985-10991. https://doi.org/10.1016/j.ifacol.2017.08.2473

[24] Catana, R. M., Cican, G., & Dediu, G. (2017) Gas Turbine Engine Starting Applicated on TV2-117 Turboshaft. *Engineering, Technology & Applied Science Research*, *7*(5), 2005-2009. https://doi.org/10.48084/etasr.1315

[25] Chunxiang, L. (2019). Nichibo Motor ShenzhenCO LTD; Multi-load-point rapid testing device for brushless motor, CN209044032U.

[26] Chengjun, C., Shelin, C., Xiaohua, K., Yang, L., Zhongmin, Y., Renwei, Y., & Chengbang, S. (2019). Measurement & Control Tech CO LTD, Brushless direct current motor performance test system, CN209342880U.

[27] Kósa, P., Kišev, M., Vacho, L., Tóth, L., Olejár, M., Harničárová, M., Valíček, J., & Tozan, H. (2022). Experimental Measurement of a UAV Propeller's Thrust, *Technical gazette*, *29*(1). https://doi.org/10.17559/TV-20201212185220

[28] Savoye, F., Venet, P., Millet, M., & Groot, J. (2012). Impact of periodic current pulses on li-ion battery performance. *IEEE Trans. Ind. Electron.*, *59*, 3481-3488. https://doi.org/10.1109/TIE.2011.2172172

[29] Hu, P., Chai, J., Duan, Y., Liu, Z., Cui, G., & Chen, L. (2016). Progress in nitrile-based polymer electrolytes for high performance lithium batteries. *J. Mater. Chem.* A, *4*, 10070-10083. https://doi.org/10.1039/C6TA02907H

[30] https://tutorials-raspberrypi.com/digital-raspberry-pi-scale-weight-sensor-hx711/

[31] https://www.rotordronepro.com/understanding-kv-ratings/

[32] https://lucidar.me/en/unit-converter/revolutions-per-minute-to-meters-per-second/

Contact information:

Tiberius-Florian FRIGIOESCU
National Research and Development Institute for Gas Turbines COMOTI,
220D Iuliu Maniu, 061126 Bucharest, Romania
E-mail: tiberius.frigioescu@comoti.ro

Teodor-Adrian BADEA
National Research and Development Institute for Gas Turbines COMOTI,
220D Iuliu Maniu, 061126 Bucharest, Romania
E-mail: teodor.badea@comoti.ro

Mihaela Raluca CODRUZ
National Research and Development Institute for Gas Turbines COMOTI,
220D Iuliu Maniu, 061126 Bucharest, Romania
E-mail: raluca.codruz@comoti.ro

Grigore CICAN
(Corresponding author)
Faculty of Aerospace Engineering, Politehnica University of Bucharest,
1-7 Polizu Street, 011061 Bucharest, Romania
E-mail: grigore.cican@upb.ro

Ionel MiNDRU
SC AUTONOMOUS FLIGHT TECHNOLOGIES R&D SRL,
152 Traian Street, Bucharest, Romania
E-mail: ionel.mindru@aft.ro